DOT/FAA/TC-15/59

Federal Aviation Administration
William J. Hughes Technical Center
Aviation Research Division
Atlantic City International Airport
New Jersey 08405

Lithium Battery Thermal Runaway Vent Gas Analysis

November 2016

Final Report

U.S. Department of Transportation
Federal Aviation Administration

NOTICE

Technical Report Documentation Page

1. Report No.	2. Government Accession No.	3. Recipient's Catalog No.
DOT/FAA/TC-15/59		

4. Title and Subtitle	5. Report Date
Lithium Battery Thermal Runaway Vent Gas Analysis	November 2016
	6. Performing Organization Code

7. Author(s)	8. Performing Organization Report No.
Thomas Maloney	

9. Performing Organization Name and Address	10. Work Unit No. (TRAIS)
U.S. Department of Transportation William J. Hughes Technical Center Aviation Research Division Fire Safety Branch, ANG-E211 Atlantic City International Airport, NJ 08405	11. Contract or Grant No.

12. Sponsoring Agency Name and Address	13. Type of Report and Period Covered
Federal Aviation Administration Office of Hazardous Materials Safety FAA National Headquarters 800 Independence Ave., SW Orville Wright Bldg (FOB10A) Washington, DC 20591	Final Report
	14. Sponsoring Agency Code ADG-1

15. Supplementary Notes

16. Abstract

Thermal runaway of lithium-metal and lithium-ion cells has resulted in numerous fires. Often the fires are fueled by the flammable gases that are vented from the batteries during thermal runaway. In addition to those installed on the aircraft, millions of lithium batteries are shipped every year as cargo. A Class C cargo compartment is equipped to have an initial concentration of 5% Halon 1301 fire-suppressing agent, followed by a residual concentration of 3% for the remainder of a flight. These halon concentrations are effective at mitigating fires involving typical cargo; however, there is concern whether these concentrations are sufficient to handle a cargo fire involving lithium batteries and to mitigate the risks of a potential explosion of the accumulated vented battery gases.

Tests were conducted to analyze the various gases that were vented from lithium cells in thermal runaway and evaluate the risk of the buildup and ignition of the gases within an aircraft cargo environment.

Small-scale tests were carried out in a 21.7 L combustion sphere in which a gas chromatograph, non-dispersive infrared, paramagnetic analyzer, and pressure transducer were used to quantify the individual gases released from lithium batteries. Once the gas constituents were quantified, tests were performed to measure the pressure increase from combustion of these gases. Large-scale tests were then conducted in a 10.8 m^3 combustion chamber, a volume comparable with that of a cargo compartment, to validate the small-scale tests and to evaluate the effect of Halon 1301 on battery vent gas combustion.

Results of the small-scale tests showed that the volume of gas emitted from cells increased with state-of-charge (SOC). Combustion of the gases showed a lower flammability limit of 10% and an upper flammability limit that varied between 35% and 45%, depending on SOC. The combustion tests also showed a maximum pressure rise of more than 70 psia at altitude or more than 100 psia at sea level.

Tests conducted at the approximately 5% halon design concentration resulted in insignificant change to the resulting pressure rise. Tests at approximately 10% concentration effectively inerted the cargo compartment such that the battery gases were unable to ignite.

The results of these tests showed that a variation in SOC affected gas volume substantially for certain cells and that a combustion event could compromise the safety of an aircraft. The Halon 1301 fire-suppression system showed minimal effectiveness against battery gases at current design concentrations of 5%.

17. Key Words	18. Distribution Statement
Lithium, Lithium-ion, Battery, Batteries, Thermal runaway, Vent gas	This document is available to the U.S. public through the National Technical Information Service (NTIS), Springfield, Virginia 22161. This document is also available from the Federal Aviation Administration William J. Hughes Technical Center at actlibrary.tc.faa.gov.

19. Security Classif. (of this report)	20. Security Classif. (of this page)	21. No. of Pages	22. Price
Unclassified	Unclassified	35	

TABLE OF CONTENTS

LIST OF FIGURES

LIST OF TABLES

LIST OF ACRONYMS

FID	Flame ionization detector
GC	Gas chromatograph
LCO	Lithium cobalt oxide
LFL	Lower flammable limit
NDIR	Non-dispersive infrared
SOC	State-of-charge
THC	Total hydrocarbon concentration
UFL	Upper flammability limit

EXECUTIVE SUMMARY

Lithium-ion and lithium-metal battery cells are known to undergo a process called thermal runaway during failure conditions. Thermal runaway results in a rapid increase of battery cell temperature accompanied by the release of flammable gas. These flammable gases will often be ignited by the battery's high temperature, resulting in a fire. In addition to the combustion of these gases as they vent, another concern is the accumulation and potential explosion of the gases.

Thermal runaway of lithium-metal and lithium-ion cells has resulted in numerous fires. Some of the notable thermal runaway events within the aircraft environment include an aircraft auxiliary power unit battery, an aircraft main battery, and one aircraft emergency local transmitter battery. In addition to those installed on the aircraft, millions of lithium batteries are shipped every year as cargo. In the event of a fire, a Class C cargo compartment is equipped to have an initial concentration of 5% Halon 1301 fire-suppressing agent, followed by a residual concentration of 3% for the remainder of the flight. These halon concentrations are effective at mitigating fires involving typical cargo; however, there is concern whether these concentrations are sufficient to handle a cargo fire involving lithium batteries and to mitigate the risks of a potential explosion of the accumulated vented battery gases.

Tests were conducted to analyze the various gases that were vented from lithium cells in thermal runaway and to evaluate the risk of the buildup and ignition of lithium battery gases within an aircraft cargo environment.

Small-scale tests were carried out in a 21.7 L combustion sphere in which a gas chromatograph, non-dispersive infrared, paramagnetic analyzer, and pressure transducer were used to quantify the individual gases released from lithium batteries. Once the gas constituents were quantified, tests were performed to measure the pressure increase from combustion of these gases. Large-scale tests were then conducted in a 10.8 m^3 combustion chamber, a volume comparable with that of a cargo compartment, to validate the small-scale tests and to evaluate the effect of Halon 1301 on battery vent gas combustion.

Results of the small-scale tests showed that the volume of gas emitted from cells increased with state-of-charge (SOC). Combustion of the gases showed a lower flammability limit of 10% and an upper flammability limit that varied between 35% and 45%, depending on SOC. The combustion tests also showed a maximum pressure rise of more than 70 psia at flight altitudes or more than 100 psia at sea level.

Tests conducted at approximately 5% halon concentration, which is a design concentration for aircraft cargo compartments, resulted in insignificant change to the resulting pressure rise. Tests at approximately 10% concentration were effective in making the cargo compartment inert, such that the battery gases were unable to ignite.

The results of these tests showed that a variation in SOC affected gas volume substantially and that a combustion event could compromise the safety of an aircraft. The Halon 1301 fire suppression system showed minimal effectiveness against battery gases at the current design concentration of 5%.

1. INTRODUCTION

1.1 MOTIVATION

Lithium-ion and lithium-metal cells are known to undergo a process called thermal runaway during failure conditions. Thermal runaway results in a rapid increase of battery cell temperature and pressure, accompanied by the release of flammable gas. These flammable gases will often be ignited by the battery's high temperature, resulting in a fire. In addition to the combustion of these gases as they vent, another concern is the accumulation and potential explosion of the gases.

Thermal runaway of lithium-metal and lithium-ion cells has resulted in numerous fires. Some of the notable fire events within the aircraft environment include an aircraft auxiliary power unit battery, an aircraft main battery, and one aircraft emergency local transmitter battery. In addition to those installed on the aircraft, millions of lithium batteries are shipped every year as cargo.

Tests have been conducted by various organizations to document the flammable gases that were emitted from cells in thermal runaway. Sandia National Labs has carried out research on the decomposition products of cells. They showed the effect of cell aging on vent gas composition and the variation of gases that are emitted at various temperatures during thermal runaway [1].

Golubkov et al. performed tests to show the vent gas composition of three lithium-ion cathode materials. They showed that the majority of the gases released from the lithium cobalt oxide (LCO)/nickel manganese cobalt and nickel manganese cobalt cathode materials were flammable. In addition, they reviewed possible mechanisms for the breakdown of the cell electrolyte into the various gas species [2].

Tests conducted at the FAA Technical Center demonstrated the effects of an aircraft cargo container explosion caused by the combustion of accumulated thermal runaway vent gas (see figure 1). A relatively small number of 18650 cells had reacted before the explosion occurred.

Figure 1. Cargo container explosion caused by lithium battery vent gases

In another FAA test, accumulated vent gases from lithium-metal cells caused an explosion in a full-scale 727 Class C cargo compartment test. The explosion caused the panels above the compartment to dislodge and bend upward into the Class E main deck compartment. The pressure rise was great enough to launch the cockpit door off of its hinges and bend the entire wall separating the cockpit from the main deck (see figure 2).

Finally, a third test involving the combustion of lithium battery vent gases was performed at the FAA. In that experiment, 400 lithium-ion 18650 cells were allowed to vent into a 10.8 m^3 chamber from a partially closed-off, oxygen-deprived, fire-resistant box. After all the cells had vented, a spark igniter was activated, resulting in an explosion with a recorded pressure rise of 29 psig. The actual maximum pressure rise from that test may have been larger, but data were recorded only at 1 Hz.

Figure 2. Aftermath of explosion of cargo compartment from lithium battery vent gases

1.2 BACKGROUND

Lithium-metal and lithium-ion cells contain an organic compound electrolyte that decomposes when a cell undergoes thermal runaway. The electrolyte consists of a lithium salt dissolved in the organic solvent. Table 1 shows a list of commonly used or potential organic solvents. The diversity of organic solvents may cause a variety in the concentrations of exhaust gas constituents. However, as shown, the majority of the components will be made up of carbon, hydrogen, and oxygen.

Table 1. Organic solvents used in lithium batteries

Ethylene carbonate $C_3H_4O_3$
Diethyl carbonate $C_5H_{10}O_3$
Dimethyl carbonate $C_3H_6O_3$
Propylene carbonate $C_4H_6O_3$
Dimethoxyethane $C_4H_{10}O_2$
Gamma-butyrolactone $C_4H_6O_2$

As the temperature increases within a lithium battery cell, the organic compound begins to react with other components of the cell. The reactions lead to the increase in cell temperature and the production of flammable hydrocarbon and hydrogen gases.

Thermal cracking, an additional possible mechanism for the conversion of organic compounds into smaller hydrocarbon molecules, occurs when sufficient heat is applied.

Halon 1301 is the “total flooding” extinguishing agent used in the aviation industry. It is among the most effective agents available for a variety of applications. Class C cargo compartments aboard aircraft are equipped with Halon 1301 systems that are designed to knock down and suppress onboard cargo fires. To do this, the system is designed to deliver a minimum initial Halon 1301 concentration of 5% and sustain a residual concentration of 3% for the remainder of a flight.

Halon 1301 has a vapor density that is approximately five times heavier than air. Because of the difference in vapor density, stratification will occur.

The effectiveness of halon at suppressing hydrocarbon fires and its ability to prevent ignition of hydrocarbons is well noted through years of use. As shown in table 2, however, a hydrogen fire is not easily controlled with Halon 1301. In addition, hydrogen is approximately 14 times less dense than air and approximately 73 times less dense than Halon 1301. The rapid stratification of hydrogen from Halon 1301 within a cargo compartment may further reduce the ability of halon to suppress or prevent combustion. Table 2 also shows that more Halon 1301 is required to prevent ignition of flammable gas buildup than is required to extinguish an existing flame.

Table 2. Effectiveness of Halon 1301 against various gases [3]

	Minimum Inerting Concentration of Halon 1301 (includes 10% safety factor)	Design Concentration of Halon 1301 for Flame Extinguishment
Hydrogen	31.4	N/A
Methane	7.7	5.0
Ethylene	13.2	8.2
Propane	6.7	5.2
Benzene	5.0	5.0

Cargo liner material covers the inside of a Class C compartment in an aircraft with the purpose of preventing the escape of Halon 1301 and smoke. The cargo liner, however, is not designed to maintain a pressure differential between the inside of the compartment and the surrounding space in the fuselage. In addition, compartments are generally built with blowout panels that become permanently dislodged in the event of a pressure differential that would occur during a rapid decompression. The pressure differential required to disturb the cargo liner or dislodge the blowout panel is 1 psi or less. Therefore, a pressure differential greater than this will compromise the integrity of the cargo compartment and its ability to maintain the design concentration of suppression agent and possibly allow smoke and gases from the fire to spread to habitable areas of the airplane.

1.3 OBJECTIVE

The purpose of this study was to analyze and quantify the various gases that are vented from lithium cells in thermal runaway and to determine the capability of the Halon concentration used in Class C cargo compartments to provide protection upon the ignition of these gases.

2. SETUP

The series of tests were split into small-scale tests and large-scale tests. The small-scale tests were conducted in a 21.7 L combustion sphere, and the large-scale tests were conducted in a 10.8 m^3 combustion chamber.

The majority of tests used an 18650-sized lithium-ion cell of LCO chemistry. Additional tests were performed in the small-scale sphere with Li-ion NiCoMn, Li-ion $FePO_4$, and Li-metal MnO_2 cells. Figure 3 shows each of the cells tested.

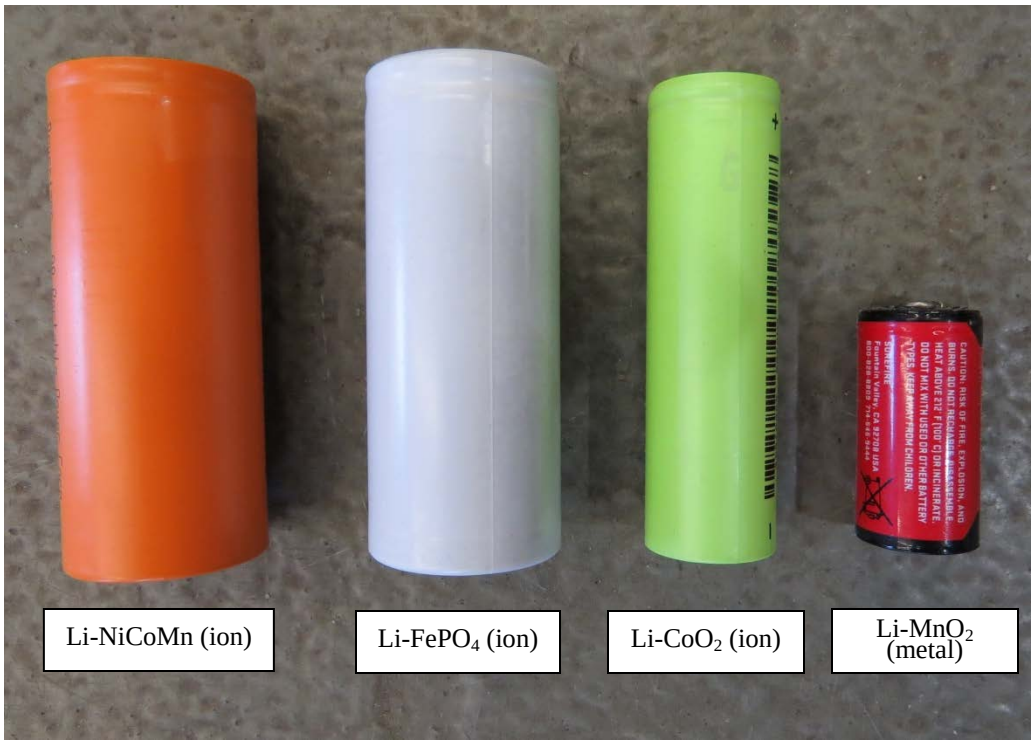

Figure 3. Cells tested in this study

A $CO/CO_2/O_2$/Halon 1301 analyzer was used in both the small-scale and large-scale tests, although the halon reading was not necessary for all of the tests. In the analyzer, the CO, CO_2, and Halon 1301 were detected with a non-dispersive infrared (NDIR) sensor, and the O_2 was detected with a paramagnetic sensor.

Similarly, a total hydrocarbon concentration (THC) analyzer was used in both the small-scale and large-scale tests. The THC analyzer used a flame ionization detector (FID) calibrated with propane.

2.1 SMALL-SCALE TESTS

The small-scale tests were performed in a 21.7 L combustion sphere (see figure 4). The sphere was constructed of steel and was closed with a hinged lid. Once the lid was closed, an O-ring between the lid and the steel body sealed the chamber. Six bolts were used to tighten the lid against the O-ring.

Figure 4. A 21.7 L test chamber for small-scale tests

The sphere was equipped with two pressure transducers. The first pressure transducer had a lower range of 0–15 psia. It was used to determine gas volumes within the sphere with partial pressure calculations. Data from the first transducer were collected at 1 Hz. A second pressure transducer, used for high-speed measurements, had a range of 0–100 psia. This pressure transducer was used to determine the maximum pressure that was created by a combustion event, and data were collected from it at a frequency of 500 Hz. A vacuum pump was attached to the chamber and was capable of evacuating the chamber pressure to 0.1 psia.

The chamber was also equipped with a 1/16″ Type-K thermocouple that was used to measure the ambient gas temperature within the chamber. The temperature within the chamber was important because a larger-than-expected rise in temperature could have skewed the gas volume calculations because pressure, volume, and temperature are dependent on each other.

The chamber was equipped with a spark igniter attached to a 10,000-volt spark generator used to ignite the unburnt hydrocarbons from the batteries in the combustion tests. Also, a 100-watt cartridge heater was wired into the chamber to initiate thermal runaway of the batteries.

In some of the tests for which gas analysis was necessary, battery gas samples were transferred from the sphere through a 15-micron particle filter and a Drierite™ water-removing filter into Tedlar® gas sample bags. The samples were then analyzed with a gas chromatograph (GC), the $CO/CO_2/O_2$/Halon 1301 analyzer, and the THC analyzer.

The GC used a HayeSep® D column for separation and a thermal conductivity detector to measure hydrogen. It used a FID to measure methane, ethane, ethylene/acetylene, propylene, propane, butene, and butane. The ethylene and acetylene coeluted from the column and were lumped together in the FID measurement. Software included with the GC was used to integrate the peaks to determine gas quantity.

Attached to the chamber was an auxiliary storage tank that was used to store battery vent gases for the small-scale combustion tests. The auxiliary tank was filled with the gases and slowly leaked into the evacuated chamber to specific concentrations. The auxiliary tank was heated to

approximately 250°F with a heater blanket in some of the tests to ensure that hydrocarbons were in the vapor phase (see figure 5).

Figure 5. Auxiliary vent gas storage chamber

2.1.1 Data Processing

Partial pressures were used to determine the volume of gas released from the cells:

$$V_{vent\ gas} = 21.7 \cdot \frac{dP_{vent\ gas}}{P_{total}} \tag{1}$$

The lower flammability limit of the sample was calculated using Le Chatelier's mixing rule, using the GC measurements of H_2, the THC analyzer measurements of the hydrocarbons, and the NDIR measurement of CO:

$$LFL_{mix} = \frac{1}{\sum \frac{x_i}{LFL_i}} \tag{2}$$

2.2 LARGE-SCALE TESTS

Large-scale tests were performed in a 10.8 m^3 steel chamber. To account for the volume of two junction boxes that were within the chamber, 10.45 m^3 was used for calculations (see figure 6). The chamber was capable of obtaining a partial vacuum to approximately 2 psia and climbing to a temperature of 750°F.

Figure 6. The 10.8 m^3 test chamber

The large-scale tests used 551 18650-sized lithium-ion cells with LCO positive electrodes. That quantity of cells was selected based on small-scale tests to produce a flammable mixture. The cells had a capacity of 2.6 Ah and were charged to 50% (1.3 Ah).

The cells were grouped together in a steel enclosure that was fitted with a chimney (see figure 7). The enclosure allowed the cells to vent into a fuel-rich environment so that premature combustion would not occur.

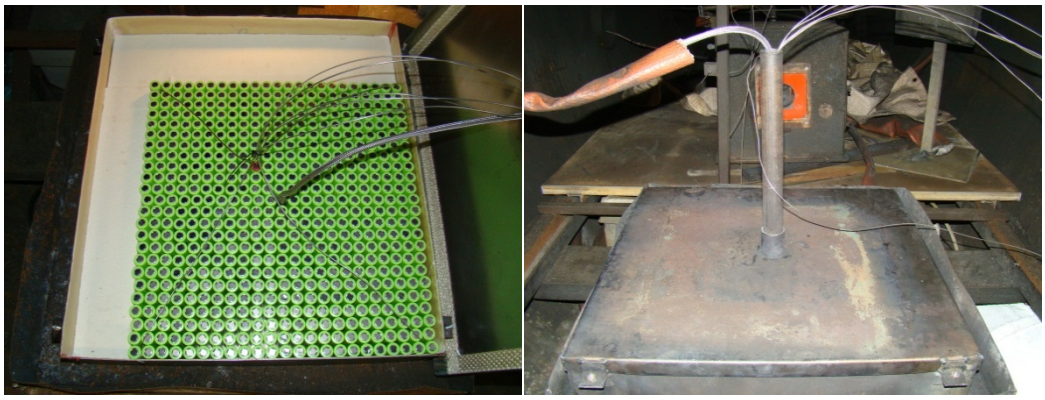

Figure 7. The 551 cell test setup with steel enclosure

The chamber was also equipped with two pressure transducers. The first pressure transducer had a lower range of 0–30 psia and was used to determine gas volumes within the chamber. Data from this transducer was collected at 1 Hz. The second pressure transducer had a higher range of 0–100 psia and was used to determine the maximum pressure achieved by a combustion event. The data from the higher range pressure transducer were collected at a rate of 1000 Hz.

The chamber was equipped with nine thermocouples spaced throughout the chamber to measure the ambient air temperatures and five additional thermocouples within the battery box to determine the progression of thermal runaway. One final thermocouple was positioned at the chimney vent to measure the temperature of the exhaust gases. All of the thermocouples used in the test were 1/16″, Type-K.

Various gas analyzers were used in the large-scale study. The gases measured include H_2, CO, CO_2, O_2, Halon 1301, and THC. An additional analyzer was used to measure the lower flammable limit (LFL). The CO/CO_2/O_2/Halon 1301 analyzer and the THC analyzer were the same analyzers used in the small-scale tests. The H_2 analyzer made by H2scan used a nickel-palladium circuit to measure hydrogen. The percent LFL analyzer was made by Control Instruments and was used to measure the proximity to LFL for the assortment of flammable gases that were present in the chamber's atmosphere. Finally, a fan was positioned within the chamber to adequately mix the gases and prevent stratification.

2.3 PROCEDURE

2.3.1 Gas Analysis (Small Scale)

One or more cells were strapped to the 100-watt cartridge heater within the sphere. The chamber was then sealed and evacuated to approximately 0.2 psia. Nitrogen was introduced into the chamber to bring the pressure back up to 10 psia. The heater was then activated and remained on until thermal runaway occurred for all of the cells. The chamber was then allowed to cool to its initial temperature. The change in pressure caused by venting was then used to calculate the volume of gas emitted. Next, the chamber was filled with nitrogen to 20 psia. Once the chamber again cooled to its initial temperature, the chamber was vented into the gas sample bag. The sample bag was then attached to the various analyzers to determine the gas concentrations. The

gas concentrations were later converted to determine the concentrations of the gases if they had not been diluted. Figure 8 shows a sample test.

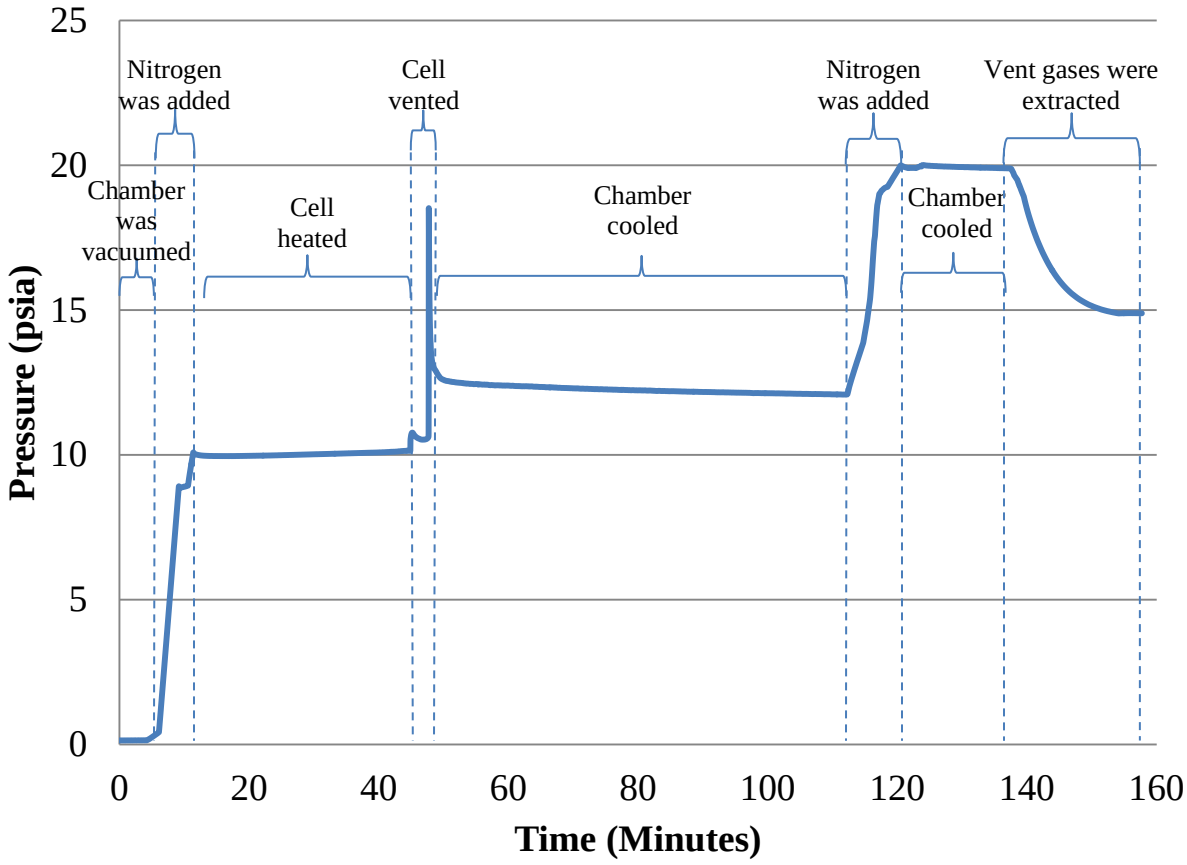

Figure 8. Example pressure profile for small-scale gas analysis tests

2.3.2 Combustion (Small Scale)

First, the group of cells was strapped together with the cartridge heater and inserted into the combustion sphere. The sphere and the auxiliary cylinder were then evacuateded to approximately 0.1 psia. The cartridge heater was then activated, and the vent gases continuously filled the sphere and auxiliary chamber until thermal runaway had completely propagated. The auxiliary chamber was then isolated with the use of manual ball valves.

The gases collected in the auxiliary cylinder were then used to conduct the combustion tests. The main chamber was again evacuated to 0.1 psia, and specific quantities of vent gases were bled into the chamber from the auxiliary cylinder followed by sufficient air to bring the vessel to 10 psia. The spark igniter was then activated, and the pressure pulse was recorded. The result was a concentration-versus-pressure-rise curve.

2.3.3 Combustion (Large Scale)

The boxed 551 cells were grouped together in the steel container with the 100-watt cartridge heater in the middle (see figure 7). Thermocouples were attached to the cells in each of the four corners and the cell adjacent to the cartridge heater. The lid was then closed, and the container was inserted into the 10.8 m^3 chamber. The chamber door was then sealed, and the chamber pressure was brought down to a predetermined pressure (depending on the halon concentration for the specific test). Halon was then released to bring the pressure to -6 psig. Thermal runaway was initiated, and once all of the cells vented, as shown by the thermocouple readings, the spark igniter was activated and the pressure rise from combustion was recorded.

3. DISCUSSION OF RESULTS

Three different series of tests were carried out to evaluate the vent gases from lithium batteries. The first series consisted of small-scale tests in the 21.7 L combustion sphere to analyze the gas constituents that were exhausted from the cells in thermal runaway. The second series of tests was also carried out in the small-scale sphere and involved combustion of the exhaust gases from one of the previously tested chemistries ($LiCoO_2$) to evaluate the pressure rise for given concentrations. Finally, the third series of tests was carried out in the large combustion chamber to verify the small-scale results and determine the effect of Halon 1301 on a combustion event.

3.1 SMALL-SCALE TESTS

3.1.1 Gas Analysis

At a higher state of charge (SOC), the overall volume of gas released from the cells increased (see figure 9). However, the gas composition varied less with a change in SOC (see figures 10 and 11). Because of the overall increase in gas volume with higher SOC, the individual quantity of each flammable gas increased significantly (see figure 12).

At a high SOC, the gases emitted from the cells generally were of lower molecular weight than at a low SOC (see figures 13 and 14). For example, there were much greater concentrations of lighter weight molecules, such as methane, ethylene, acetylene, and propylene in the 80% SOC vent gas. The 30% SOC showed a large elongated peak later in time, representing a larger molecular composition. This indicated that the electrolyte within the cell that had a relatively large molecular weight broke down further at a higher SOC.

The LFL was calculated using Le Chatelier's mixing rule for each SOC (see figure 15). The calculated LFL remained approximately constant for SOC greater than 40%. Below 40%, the LFL increased, mainly because of the reduced hydrogen composition. Based on the volume and LFL measurements, the number of cells required to create a flammable gas mixture in an empty AKE cargo container ($153ft^3$) was determined (see figure 16).

As with the LCO chemistry, $LiMnO_2$ and LCM also produced a significant quantity of flammable gas. The gases from $LiFePO_4$, however, were far less flammable (see figure 17).

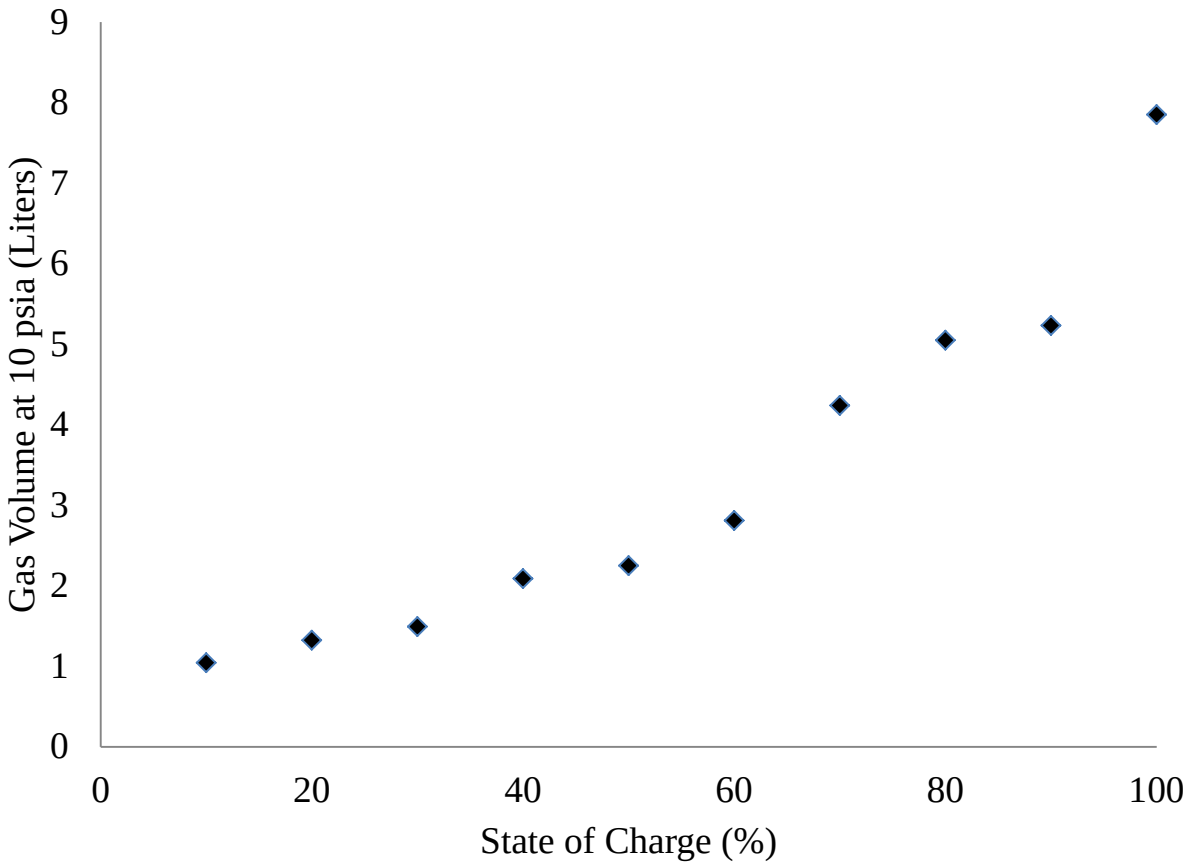

Figure 9. Gas volume emitted from 18650 $LiCoO_2$ cell

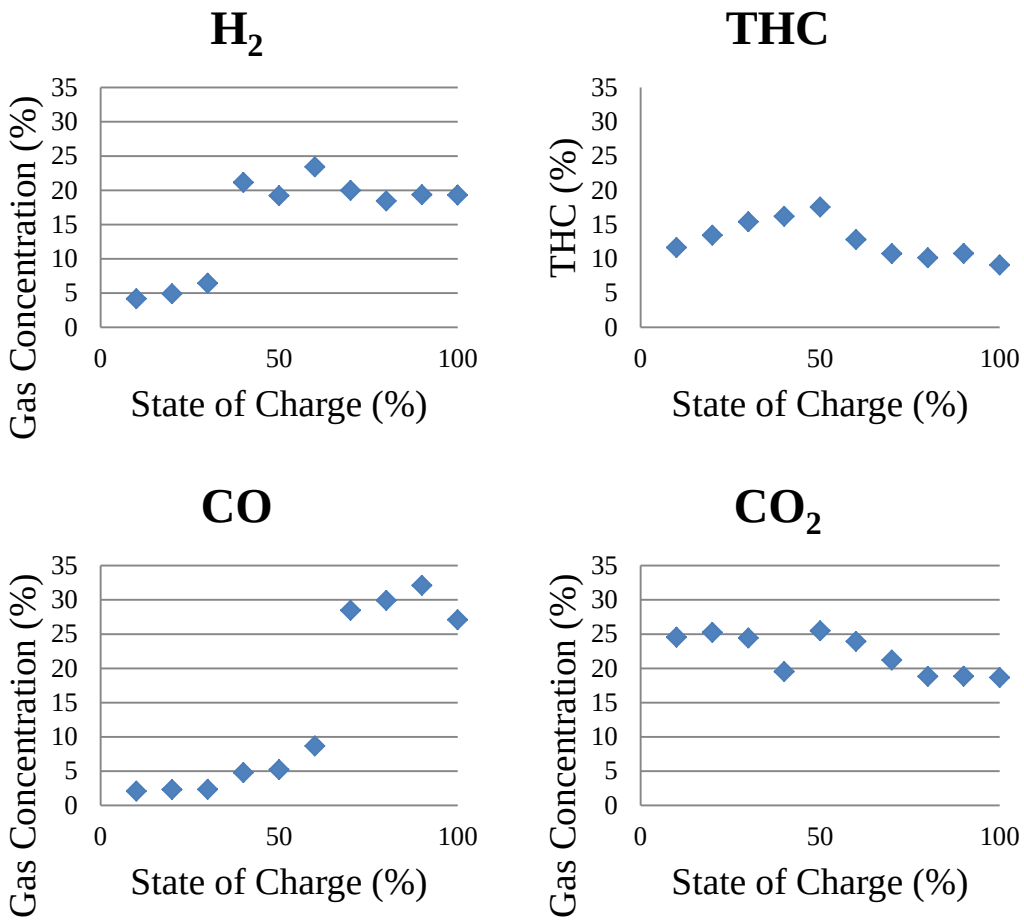

Figure 10. Major gas species concentrations for $LiCoO_2$ 18650 cells

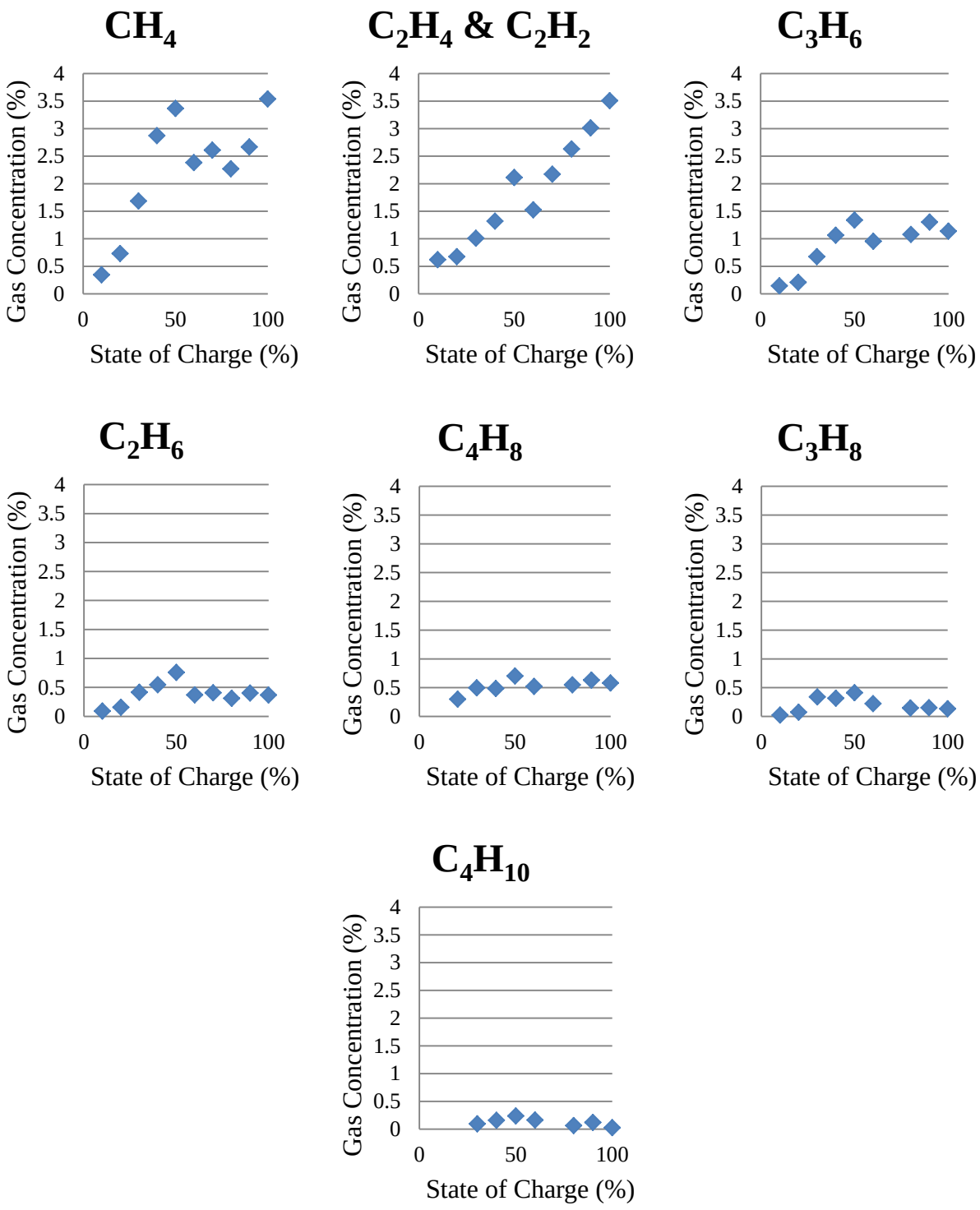

Figure 11. Individual gas species concentrations for $LiCoO_2$ 18650 cells

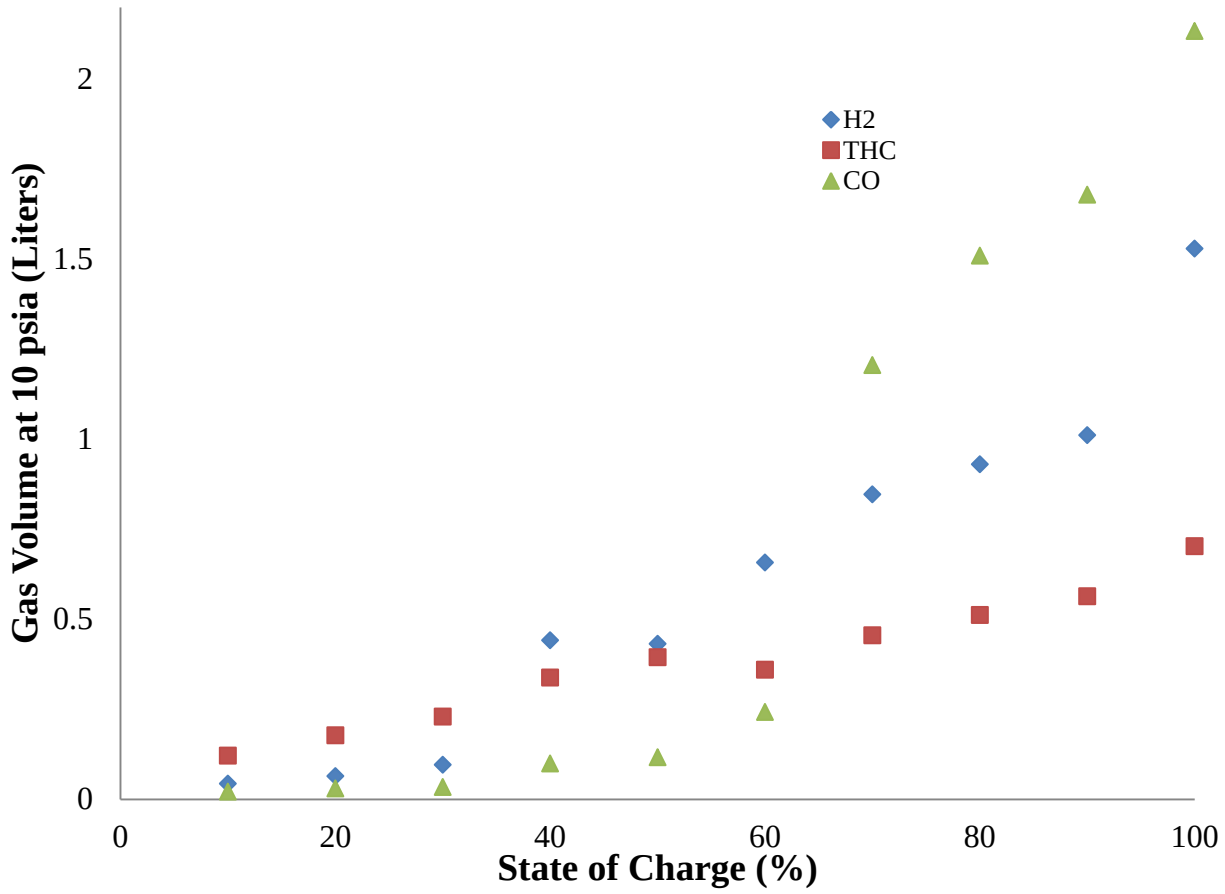

Figure 12. Flammable gases emitted from LiCoO2 18650 cells

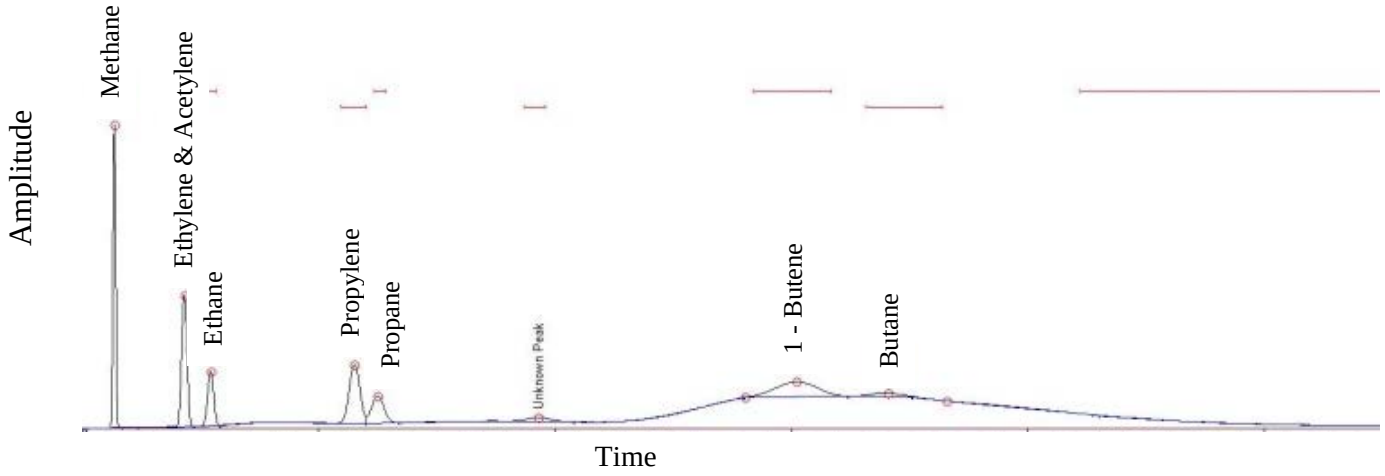

Figure 13. The 30% SOC $LiCoO_2$ cell GC chromatogram

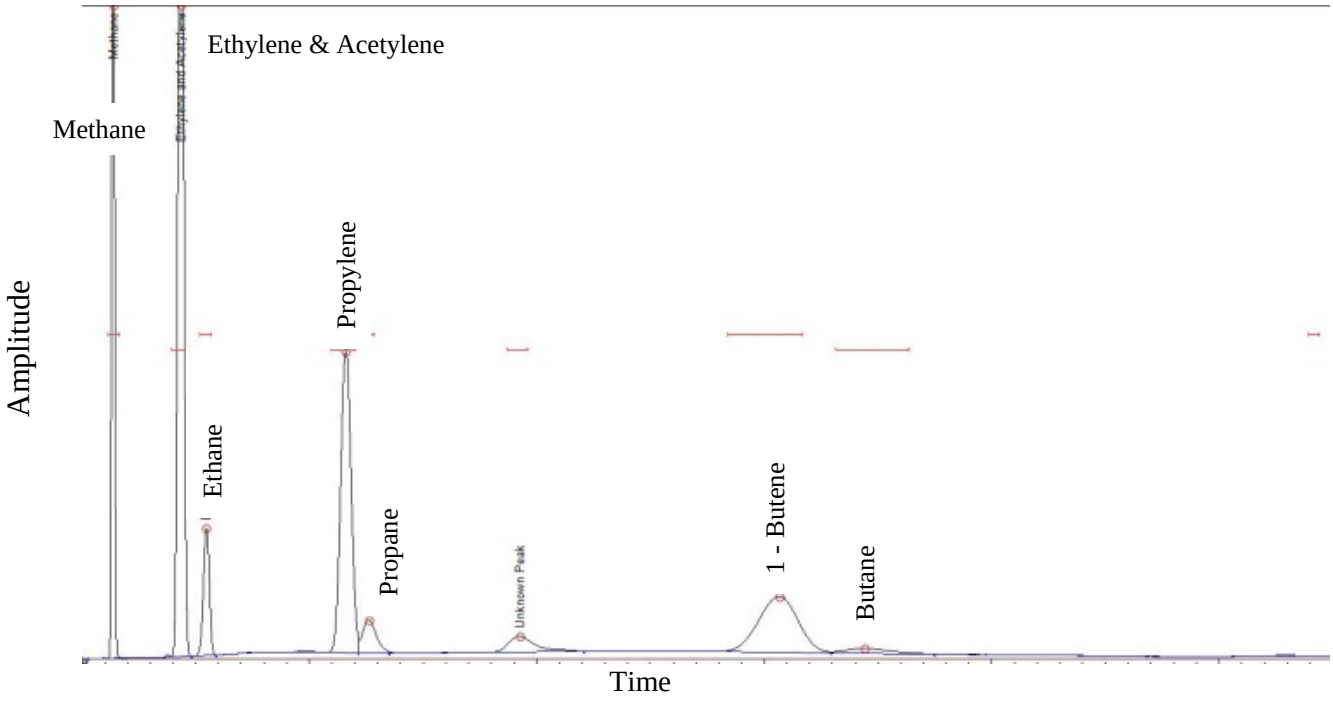

Figure 14. The 80% SOC $LiCoO_2$ cell GC chromatogram

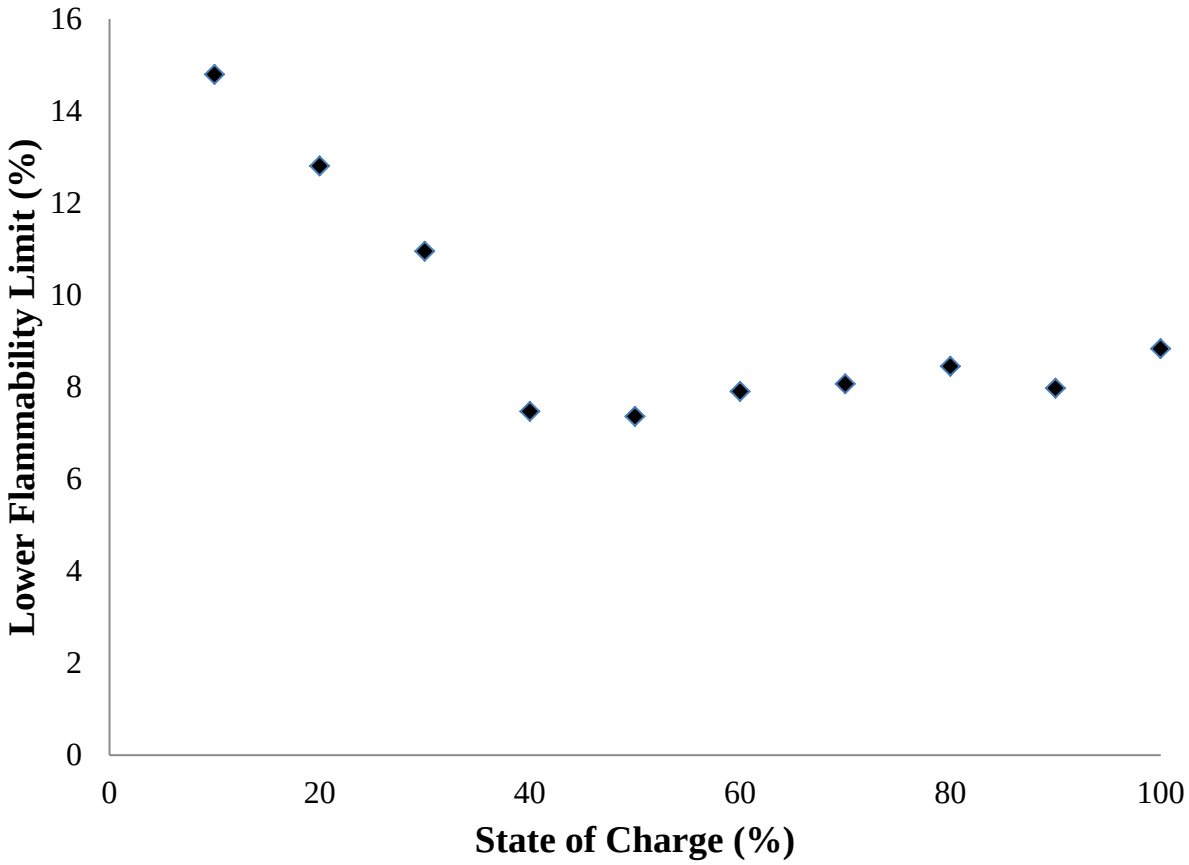

Figure 15. LFL calculated from Le Chatelier's mixing rule

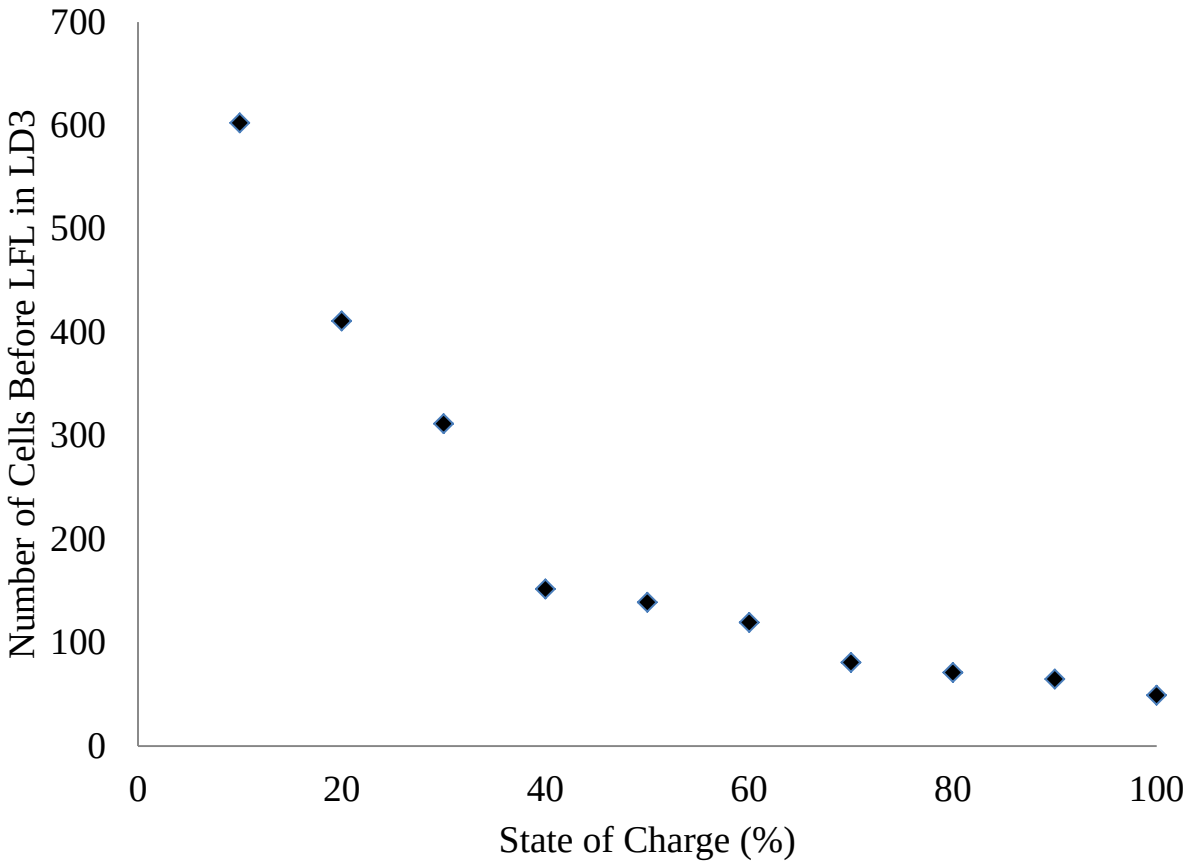

Figure 16. Number of cells required to create explosive mixture in empty AKE

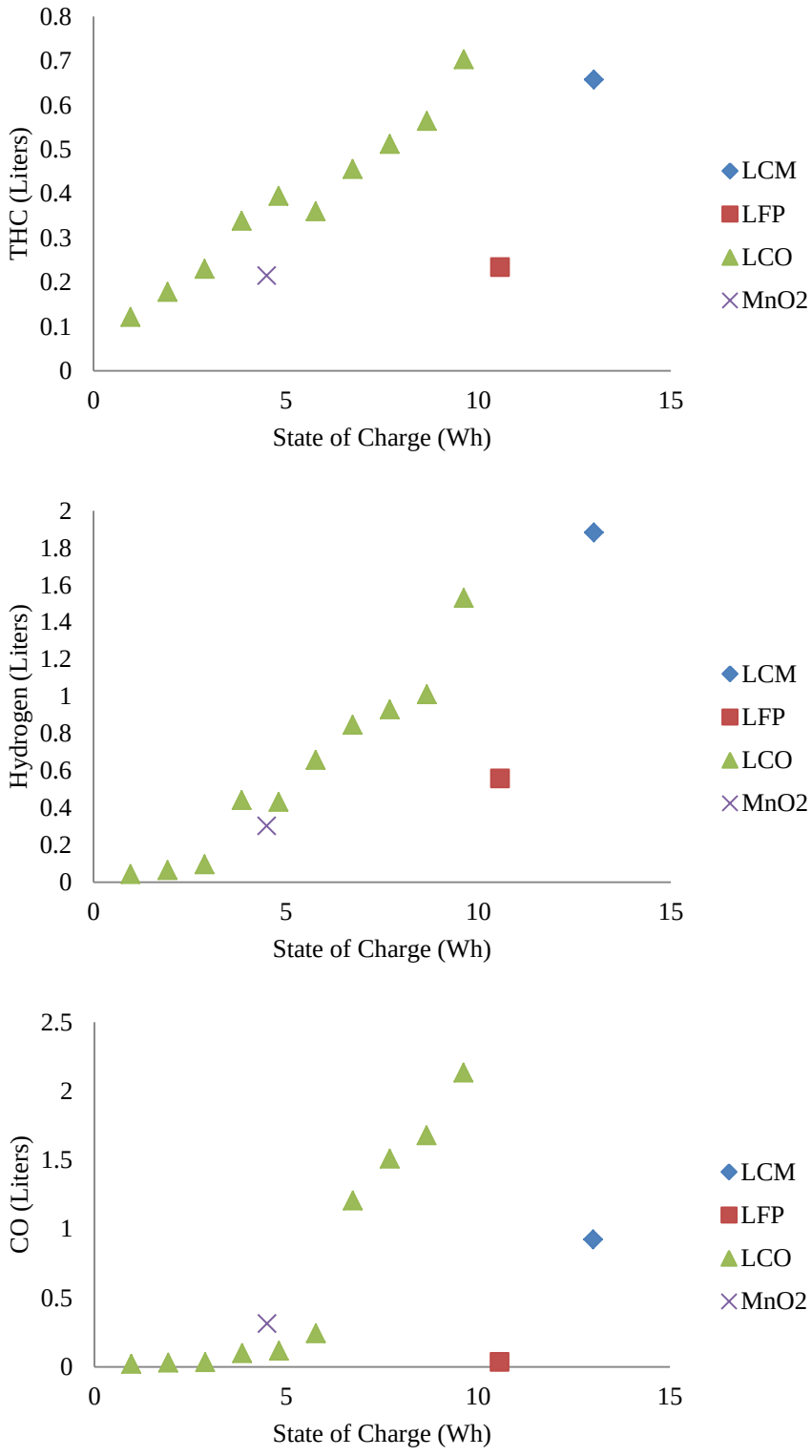

Figure 17. Flammable gases for various cell chemistries

3.1.2 Combustion

The results of the small-scale combustion tests for the 50% and 100% SOC cases showed a maximum pressure rise from a battery gas concentration of 21.47% and 25%, respectively (in air). Figure 18 shows the flammability envelope for the vent gases. When the SOC was increased from 50% to 100%, the LFL remained approximately constant, but the upper flammability limit (UFL) increased from approximately 35% to 45%. The increased UFL may be attributed to the increase in carbon monoxide at a higher SOC. The LFL results closely matched the predicted LFL from Le Chatelier's mixing rule.

Figure 19 compares the pressure rise from the tests that used vent gases stored in the pressure chamber with tests that used cells venting directly into the sphere. It was observed in the figure that the two cases produced nearly the same pressure pulse.

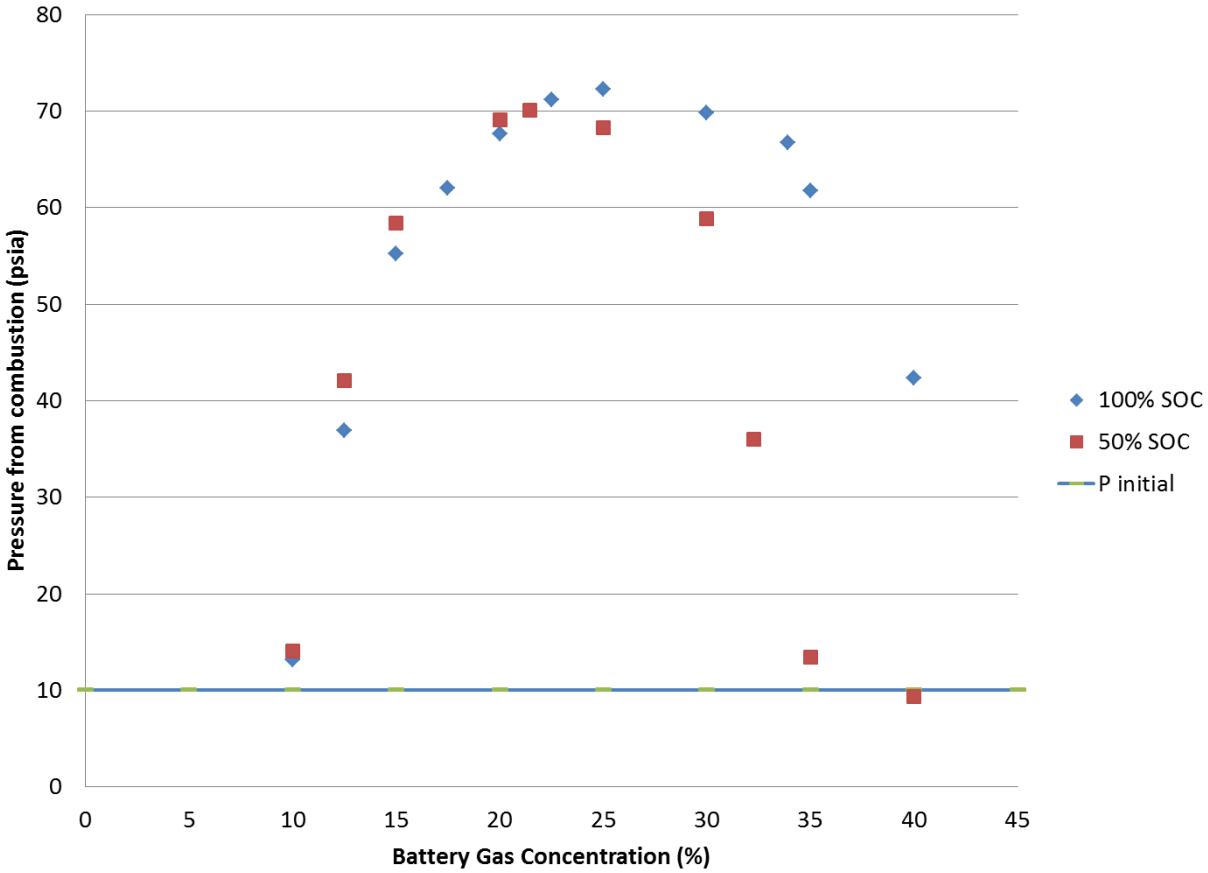

Figure 18. Pressure rise for various concentrations of battery vent gases

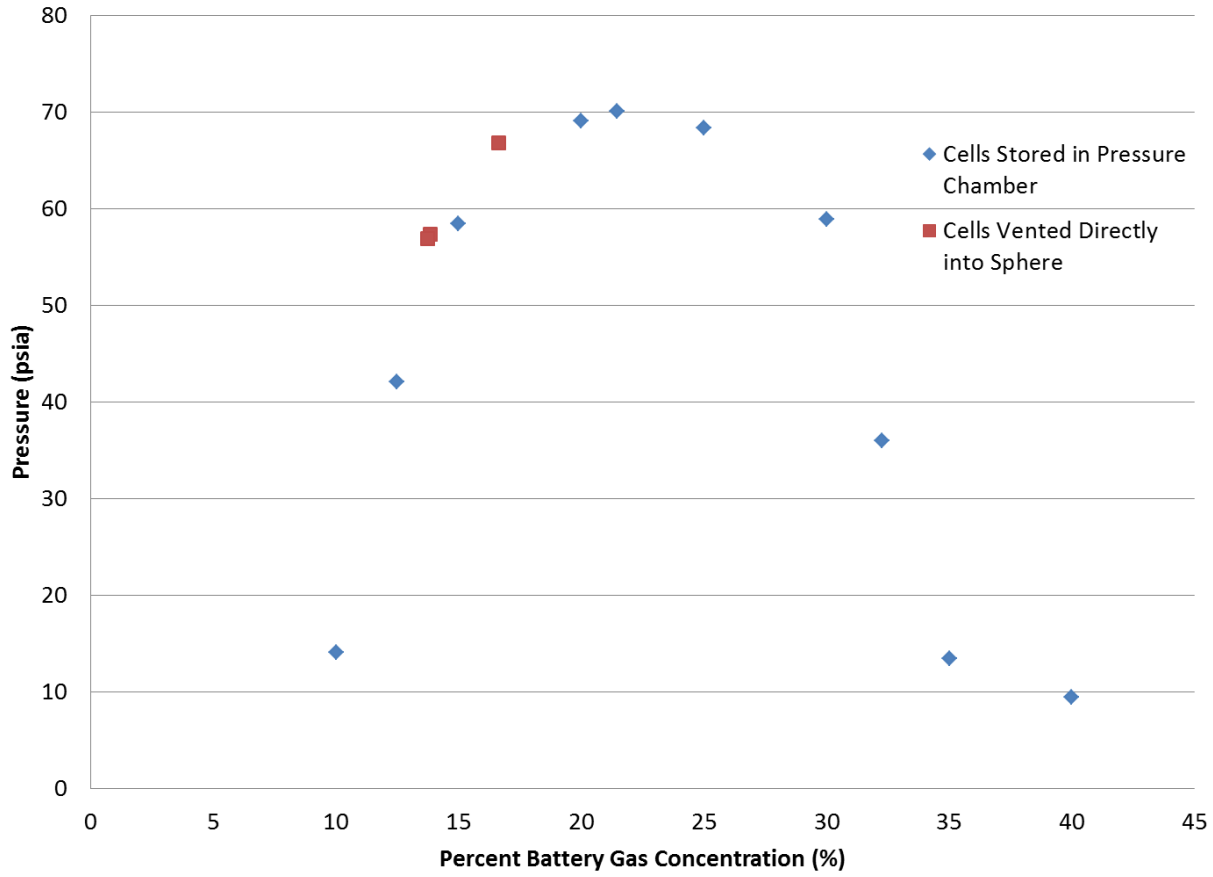

Figure 19. Comparison of pressure rise from cells vented directly in sphere and cells vented into storage chamber

3.2 LARGE-SCALE TESTS

The large-scale test results in the 10.8 m^3 chamber showed that the small-scale results were a reasonable predictor for the large-scale tests (see table 3). However, the concentrations of flammable gases were slightly higher for the large-scale test. This could be because the higher temperatures reached during the thermal runaway reactions caused greater evaporation and breakdown of the electrolyte.

Table 3. Gas concentrations from test without suppression

	Predicted Concentration from Small-Scale Tests	Actual Concentration (No Halon)	Actual Concentration (5.28% Halon)	Actual Concentration (10.43% Halon)
THC	2.08%	2.5%	2.77%	3.2%
H_2	2.27%	2.74%	3.5%	3.54%
CO	0.61%	1.4%	1.5%	2.04%
CO_2	3%	3.97%	3.42%	4.73%

Pressure prior to ignition for the 5.28% halon test shows how partial pressures were used to predict concentrations ahead of time (see figure 20). Figure 21 shows the gas concentrations from an analyzer used to verify the predicted gas concentrations.

A pressure rise to 70 psia was generated in the test without halon suppression. The concentration of 5.28% halon failed to prevent combustion of the vent gases, and a pressure similar to the pressure from the test without suppression was generated (see figure 22). However, the halon slowed the rate of pressure rise. Suppression was successful at a concentration of 10.43%. An additional test was performed with 3% halon; combustion also occurred, but the pressure peak was not recorded.

Figure 23 shows the average temperature from the chamber thermocouple during the combustion event.

The percent LFL reading for the test with 5.28% halon shows that an empty cargo compartment can change from normal to explosive in as little as 20 minutes (see figure 24). A loaded cargo compartment would become explosive in a fraction of the time because of the reduced free volume.

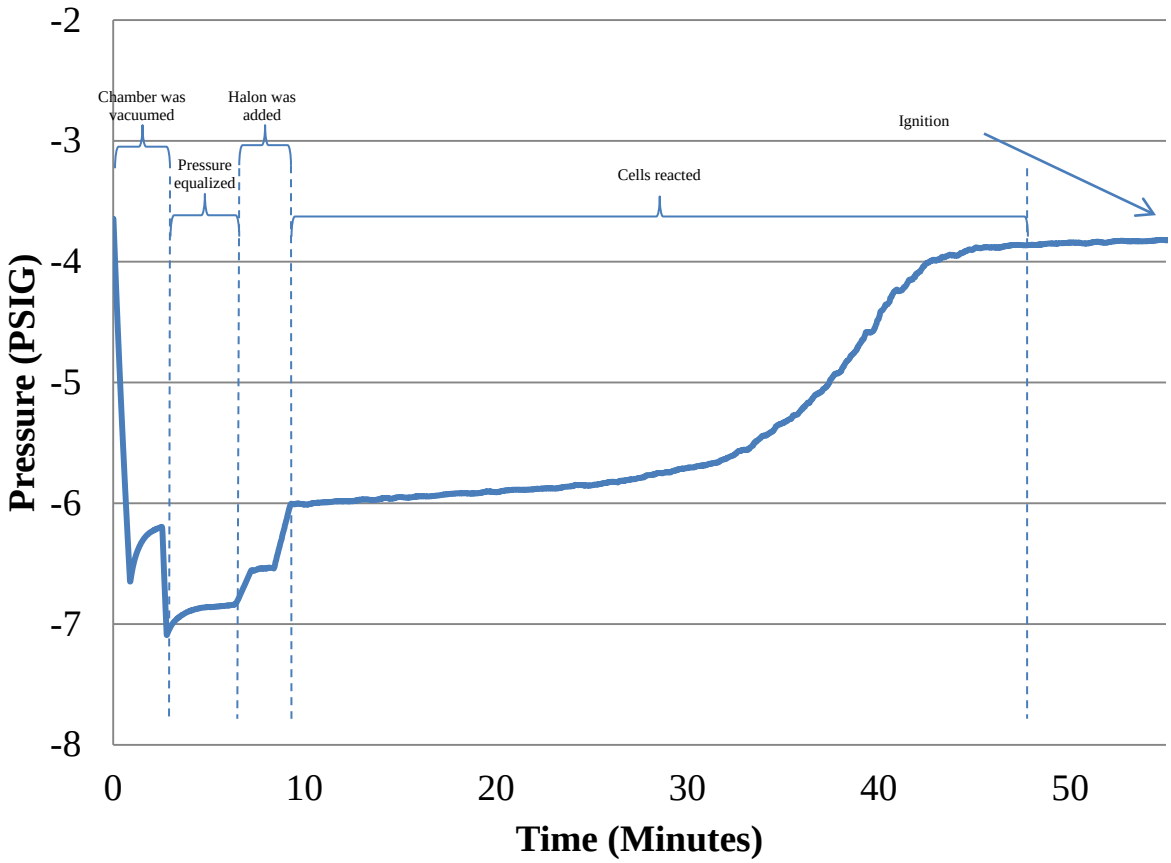

Figure 20. Pressure curve before ignition, 5.28% halon

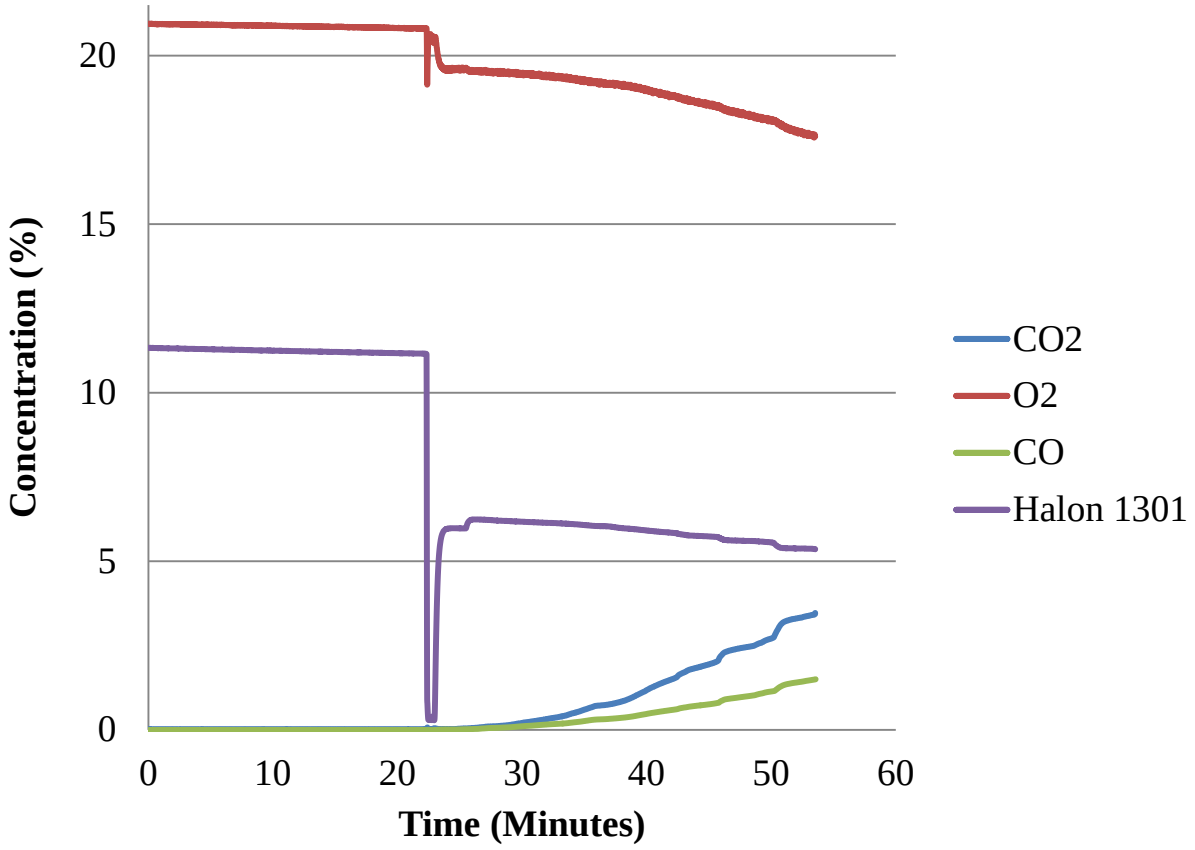

Figure 21. Gas readings for test with 5.28% halon

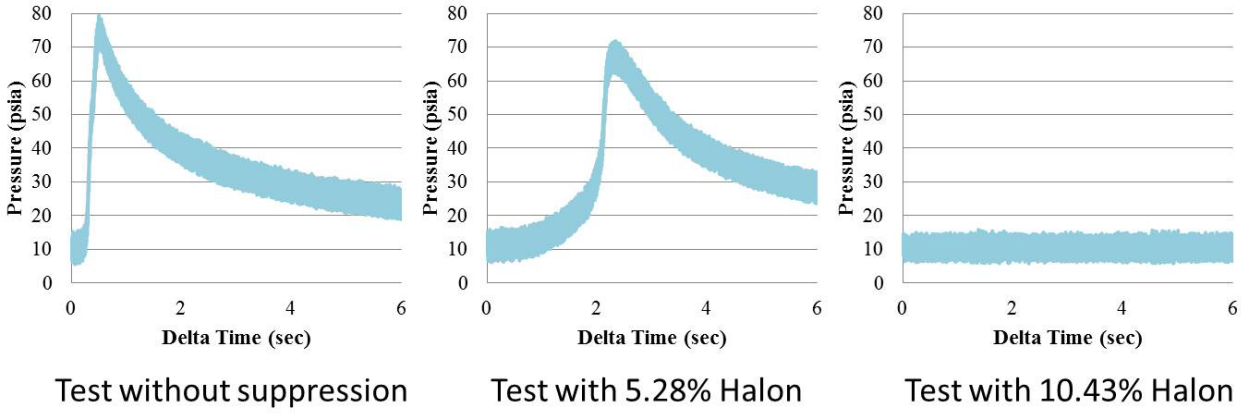

Figure 22. High-speed pressure profile for combustion of three halon concentrations

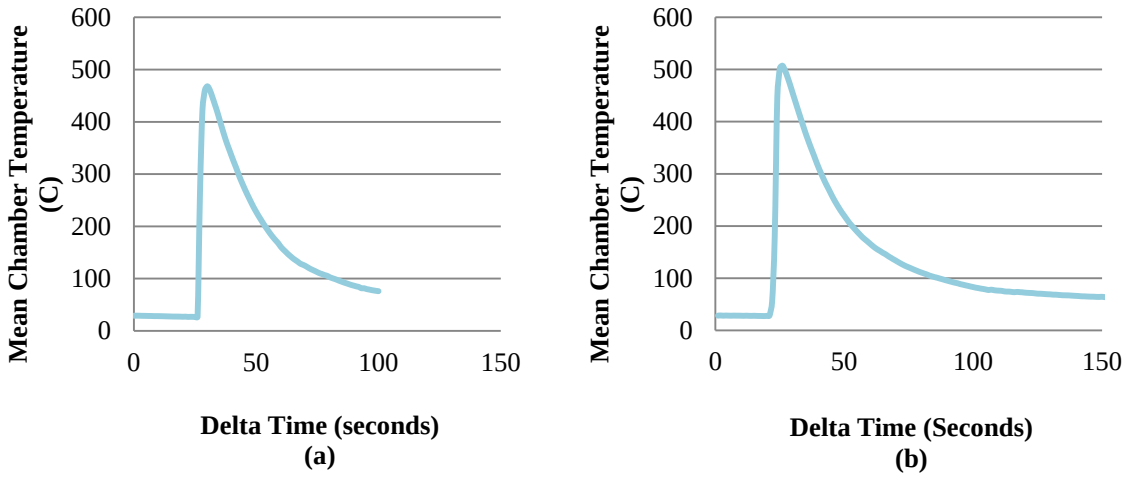

Figure 23. The (a) Baseline test without suppression and (b) test with 5.28% halon

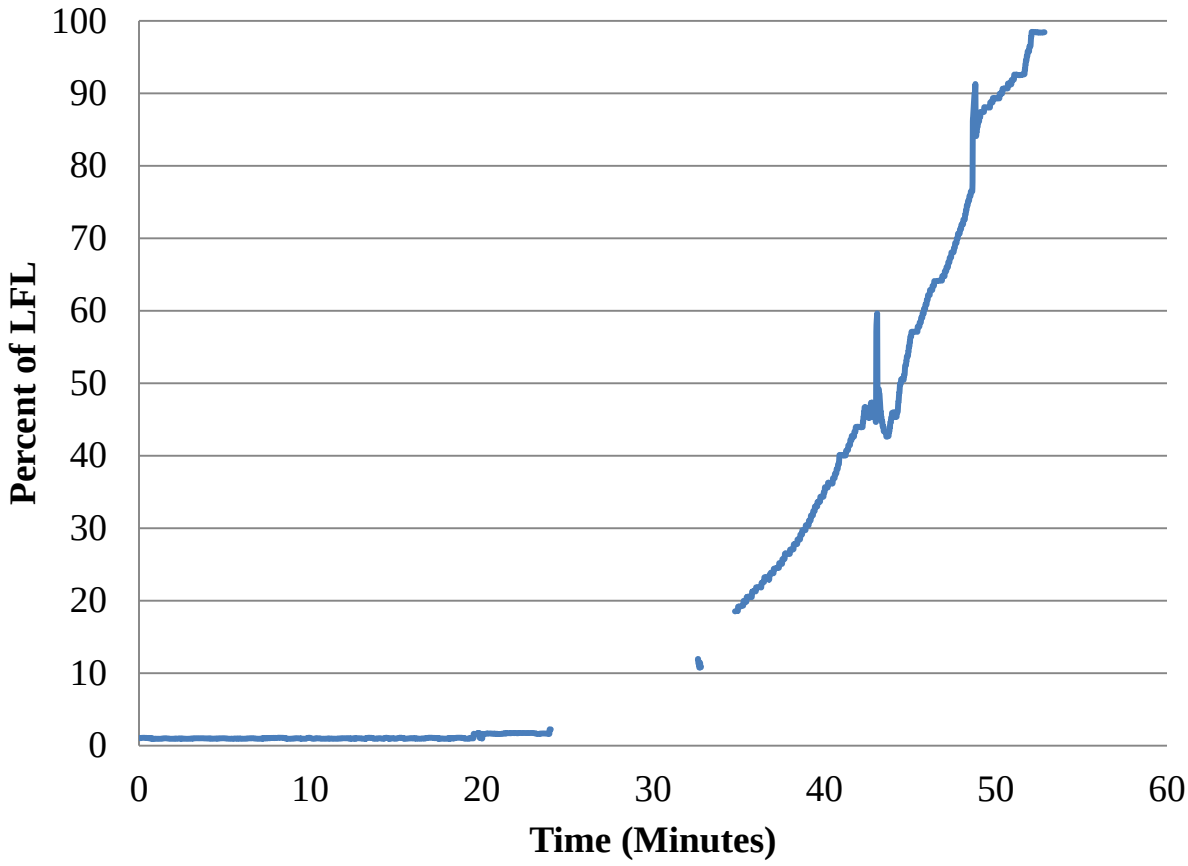

Figure 24. LFL reading from LFL analyzer for test with 5.28% halon

4. SUMMARY OF RESULTS

Lithium-ion and lithium-metal cells in thermal runaway vent a variety of flammable gases. For the lithium-ion cells, the quantity and composition of the gases vary with SOC. Higher SOC produces a greater volume of gas in the cells tested along with a wider flammability range. Hydrogen, hydrocarbons, carbon monoxide, and carbon dioxide were the most abundant gases produced.

At a higher SOC, the battery electrolyte breaks down further into smaller, more lightweight molecules.

The small-scale tests showed that cells at a higher SOC not only produced a greater volume of vent gas, but that the vent gas was also more flammable.

The small-scale tests underestimated the gas concentrations of the large-scale tests, possibly because of the greater temperatures that were reached.

Halon 1301, at its design concentration of 5% and 3%, was not sufficient to prevent an explosion of accumulated battery vent gases, and a cargo compartment had the potential to become explosive in a relatively short amount of time.

The sudden pressure rise of a partially suppressed lithium battery gas combustion event would cause more than enough pressure to dislodge the pressure relief panels. Once the panels or cargo liner is dislodged, the cargo compartment would no longer be able to maintain the required halon concentration, which could result in an uncontrolled fire. In addition, smoke and gases would leak into other parts of the aircraft and cause an additional hazard.

5. REFERENCES

1. Roth, P.E., Crafts, C.C., Doughty, D.H., and McBreen, J. (2004). "Advanced Technology Development Program for Lithium-Ion Batteries: Thermal Abuse Performance of 18650 Li-Ion Cells." Retrieved from http://prod.sandia.gov/techlib/access-control.cgi/2004/040584.pdf.

2. Golubkov, A.W., Fuchs, D., Wagner, J., et al. "Thermal-Runaway Experiments on Consumer Li-Ion Batteries With Metal-Oxide and Olivin-Type Cathodes." Retrieved from http://pubs.rsc.org/en/content/articlehtml/2013/ra/c3ra45748f.

3. Grant, C.C. (2015). Halon Design Calculations. In Hurley, M.J., Gottuk, D.T., Hall, J.R. Jr., et al. (Eds.). *SFPE Handbook of Fire Protection Engineering (5th ed.)*. pp. 1450–1482. New York, NY: Springer.